Università degli Studi di Firenze

DOTTORATO DI RICERCA IN
" Medicina Clinica e Sperimentale"

CICLO XXIV scuola in medicina interna sperimentale e applicata

COORDINATORE Prof. Giacomo Laffi

TITOLO:
"Effects of Age and Gadoxetic Acid on quantitative DW Imaging of the liver"

Settore Scientifico Disciplinare MED/36

Dottorando	**Tutor**
Dott. ssa Silvia Pradella	Prof. Stefano Colagrande

Anni 2009/2012

Index

Abbreviations:

CT: Computed Tomography

MR: Magnetic Resonance

I: Imaging

RECIST: Response Evaluation Criteria in Solid Tumors

DWI: Diffusion-Weighted Imaging

HU: Hounsfield Unit

CA: Contrast Agent

ADC: Apparent Diffusion Coefficient

PF: Perfusion Fraction

D: Diffusion Coefficient

D*: Fast Diffusion Coefficient

Gd-EOB-DTPA: Gadoxetic Acid

ROI: Region of Interest

1.Preface

1.1. *New technologies applications*

Progress in therapies, should be matched with progress in radiology imaging. For instance, morphological information in the follow up CT/MRI for cancer now seems to be inadequate.

The Response Evaluation Criteria in Solid Tumors (RECIST), is described in several articles and recommended for estimating tumor response to therapies based on the lesion size [1]. The RECIST assessment with morphologic imaging techniques, such as CT or MRI, has limitations mainly due to the morphological evaluation and in differentiating necrotic tumor or fibrotic scar from residual tumor tissue. Furthermore, some of the new targeted therapies are cytostatic rather than cytoreductive. In these applications successful treatment does not reduce the tumor size, and, therefore, new issues on imaging techniques rise [2].

New Imaging applications such as Diffusion, Spectroscopy and Perfusion attempt to provide quantitative and functional data.

Perfusion, in particular, is known since the '80, after the introduction of CT technology, when Leon Axel, first proposed a method for determining tissue perfusion from dynamic contrast enhanced CT data [3]. For many years, this application has not evolved but, nowadays, the possibility of rapid Imaging with multi-slice CT and the availability of more sophisticated analysis software made the Perfusion Imaging with CT possible. Its applications in the neurological field and body Imaging is part of daily practice.

As well, Diffusion MRI (DWI) is a method which came into existence in the mid-1980s [4-5]. This application allows the mapping of the diffusion process of molecules, mainly water, in biological tissues, in vivo and non-invasively.

Diffusion, Spectroscopy and Perfusion have been proposed, in oncology, in order to find an Imaging correlate for tumor characterization (to discriminate benign and malignant lesions) and , at the same time, an indicator of tumor aggressiveness. Moreover, the information provided can be useful for a functional assessment of tumor response to therapy. The ability to identify changes in a tumor's perfusion offers the potential to predict growth or regression. With this data, clinicians could offer more tailored treatment, which might ultimately improve patient's outcomes.

In light for this, recently the Imaging is focusing on new fields. Modern software, which still have to be validated, are now available, promising to provide quantitative and functional information.

During my PhD, I mainly studied the Perfusion and the Diffusion, while I could not study the Spectroscopy, failing an adequate equipment, which remains one of the most promising MRI applications.

• Perfusion is based on the assessment of the contrastographic dynamic curves and can identify areas of increased or reduced blood perfusion (for example neoplasms may show an early and strong contrast enhancement mainly due to the neoangiogenesis processes). Highly vascularized tumors are often associated with a poor prognosis and high capability of metastasis. Perfusion is able to detect early changes in the microcirculation. Several studies demonstrated that in pathological conditions, such as cirrhosis, perfusion parameters change significantly (decrease in portal and hepatic flow, increase in arterial perfusion and the mean transit time) depending on the severity of the disease (related to Child-Pugh) [6]. There is a relationship between the presence of tissue modifications and Perfusion changes. There are many available CT software dedicated to Perfusion Imaging based on the hypothesis that the concentration of the contrast agent (CA) and variation of density attenuation values, measured in Hounsfield Units (HU), are directly proportional. Recording the first pass of the CA bolus through the vascular system we can estimate the time-attenuation curves. The data obtained are theoretically comparable and reproducible.

Then, the parameters such as BF (Blood Flow: blood flow velocity), BV (Blood Volume: blood volume), PS (Permeability Surface: interstitial permeability), and MTT (mean transit time: mean transit time of the contrast in the analyzed volume) can be obtained. High BF correlates with the presence of a low resistance to the flow due to arteriovenous shunts, which determines an increase in the flow velocity and consequently a low MTT. A high BV may indicate a vascular angiogenesis and a high PS indicates an increase in capillary permeability typical of tumor tissues. This method, therefore, appears to be useful for the characterization of lesions, therapeutic planning and monitoring of cancer therapies [6].

• Diffusion-weighted Imaging can study water diffusion properties of examined tissue. This approach is based on the measurement of Brownian motion of molecules. It has been known for a long time even though superficially, that nuclear magnetic resonance is capable of quantifying diffusional movement of molecules. It is possible to

use this diffusion property as a probe to study the structure of spatial order in living organs noninvasively [7].

•   Magnetic resonance spectroscopy (MRS) is a non-invasive technique that allows to obtain biochemical information from tissues and organs. This method provides the relief and measurement of known metabolites present in the studied tissue volume. The signal, arising from different isotopes (H, P, C13 etc.), is recognizable because isotopes resonate at known frequencies when placed in a magnetic field. The equipment necessary for this type of study is a high field (1.5 / 3 T) and the related software [8].

1.2.   Role of CT and MRI

I'm a slow walker, but I never walk back. [1]

Perfusion can be studied in both CT and MRI. The first field of Perfusion application was the Neurology Imaging but promising employments are for Cardiology and Oncology Imaging.

The basis for the use of Perfusion in Oncology is that the microvascular changes in angiogenesis are reflected by increased tumor perfusion in vivo.

The CT Perfusion is based on "the principle of central volume" (which put in correlation blood flow, blood volume and mean transit time in the equation: BF= BV/MTT) . The assumptions are that the contrast agent:1) completely mixes with the blood, 2) during the first pass is completely intravascular, 3) CT attenuation values reflects accurately the concentration of the contrast medium, and 4) through the vascular bed this does not cause hemodynamic or physiologic changes.

Because of its linearity, CT is of advantage on MRI, where this relationship does not exist [9]. Therefore, CT employment has gained wider acceptances, than MRI. At the beginning of my PhD, our group studied this technique on oncologic patients with the aim at finding a possible application of CT Perfusion during the early monitoring of chemotherapy. Unfortunately, the first data showed the following issues:

- lack of reproducibility,

- high radiation doses,

---

[1] Abraham Lincoln

- need of high CA flow.

As a consequence, we decided to interrupt the study and focus our efforts in validating the Diffusion.

In fact, Diffusion, is of particular interest because it allows to examine, at molecular level, what happen in the tissues, providing data that might be important in the early diagnosis of diseases.

2. Personal Experience

2.2. *Abstract*

Purpose:

The purpose of this study was to verify the influence of age and Gadoxetic Acid (Gd-EOB-DTPA; Primovist, Bayer-Schering, Berlin, Germany) on DWI-related parameters: apparent diffusion coefficient (ADC), perfusion fraction (PF), diffusion and fast diffusion coefficient (D and D*) using the Le Bihan IntraVoxel Incoherent Motion method.

Materials and Methods:

To investigate the influence of age on the diffusion parameters, forty healthy adult volunteers, divided into four age groups, were prospectively submitted to a breath-hold MR-DWI (two b values 0–300 and 0–1000 s/mm^2 and a free-breath multi-b acquisition 16 b values, 0–750 s/mm^2) -to investigate the influence of Gadoxetic Acid on the diffusion parameters, twenty-four consecutive patients, were prospectively submitted to MR-DWI acquisition before and after gadoxetic acid administration. The patients were divided into four groups according to the time at which the DW sequence was repeated (5, 10, 15, 20 minutes after contrast agent administration).

Quantitative analysis was performed by two observers with manually defined regions of interest (ROIs), in the most homogeneous portion of the right liver lobe. The mean and standard deviation (SD) were calculated in each group/patient for every DWI related parameter.

Results:

ANOVA showed no significant differences among age groups (p n.s.). Moreover, D, D*, PF, and ADC did not show any significant difference before and after contrast agent administration, at any time.

Conclusions:

No significant correlation between subjects' age and DW

I parameters were observed, both in breath-hold and freebreath acquisitions.

It is possible to perform DW acquisitions after gadoxetic acid administration without any significant variation in the values of DW-related parameters.

2.3. Keywords

DWI; quantitative DWI; ADC; Gd-EOB-DTPA; Primovist; gadoxetic acid, age

2.4. Introduction

Diffusion-weighted MRI is an emerging technique even for body applications [10,11]. The calculation of the apparent diffusion coefficient (ADC), by means of MR-DWI, allows the quantification of the combined effects of molecular Brownian motion of water within tissues and perfusion [5,12]. Although the DWI has been proposed to differentiate benign from malignant lesions or stage hepatic fibrosis [13,14] soon many limitations arose, especially for the liver (e.g. low spatial resolution and signal-to-noise ratio, the great sensitivity to movement and to magnetic susceptibility artifacts, and the lack of reproducibility of the obtained data). DWI is routinely used for focal liver lesions detection, but not for their characterization. Nowadays, its role in assessing the effects of therapies, is still challenging [15]. The potentiality of DWI is still controversial due to technical and physiological factors affecting ADC measurements, such as the b factor, the time of echo (TE), the site and size of sampling methods, the temperature, the diffusional intravoxel incoherent motion (IVIM) related to perfusion, the modality of acquisition (breath-hold, BH, free-breath FB, echo-navigator) [12,16–27]. Moreover, difficulties related to intrinsic sensitivity to motion and magnetic susceptibility of DW sequences should also be taken into consideration.

Furthermore, the effects of patient's characteristics (e.g. age) or differences related to the type of examination (influence of the contrast agent) on DWI has not been fully investigated. I think it is important to investigate these variables in order to better understand which is the reproducibility and reliability of DWI parameters.

In light of this, during the last years we studied the influence of age and contrast agent on DWI main quantitative parameters: ADC, PF, D and D*.

As known, in clinical practice, DWI is usually added to acquisition protocols before CA administration, which are, in hepatic evaluations, often liver-specific Gd-chelates [28]. The most recent one of these agents is the gadoxetic acid disodium (Gd-EOB-DTPA; Primovist, Bayer- Schering, Berlin, Germany), is characterized by biliary excretion close

to 50%, which allows liver specific phase acquisitions after 10–15 minutes. The whole examination may be concluded in a single step without interruption. Therefore, a time interval between the 5th and the 15–20th minute after the CA administration, exists. In order to optimize/reduce the examination time, an "inverted protocol" in which the T2w sequences are performed after gadoxetic acid administration, can be adopted. This approach may lead to spare time during the interval between the dynamic and delayed hepatobiliary phases [29-31]. Trough assessing any possible change in DWI parameters, due to CA, we suggest the opportunity of sparing time by obtaining DWI after CA administration instead of before.

2.5. *Materials and Methods*

The study protocol was approved by the investigation and Ethics Committee of our institution for volunteers aware of aim and nature of our prospective study. Each of them provided a written consent before beginning the examination, in accordance with the principles of the Declaration of Helsinki (revision of Edinburgh, 2000). To study the influence of CA, the Institutional Review Board approval was waived because of the characteristic of the study. In fact, we added, to our standard protocol, only a DWI acquisition after CA administration. Each patient signed the permission form for CA administration where contraindications were specified, as standard procedure. All examinations were performed after six hours fasting.

Patients

Within one year (2009-2010) we prospectively included forty healthy adult volunteers undergoing abdominal MR-DWI. Patient's age covered a range included between 18 and >65 years. The patients were divided into four groups, ten each one, as follows: 18–30 (group A), 31–45 (group B), 46–65 (group C), >65 years (group D). The inclusion criteria for this study were as follows:

-no history of illegal drug use or alcohol abuse,

-normal liver on ultrasound study (no focal or diffuse liver disease, including

mild steatosis)

-normal liver function tests and no history of abdominal surgery.

During two months of 2011, we prospectively included all patients, with or without cirrhosis, requiring liver MR examinations with the administration of gadoxetic acid in

order to detect/exclude, characterize, or follow-up focal lesion(s). In this study group we performed a DWI sequence before and after gadoxetic acid administration. The patients were divided into four groups, according to the time at which the DWI sequence were repeated (after 5, 10, 15, and 20 minutes after the CA administration). Uncooperative patients were excluded from the study.

MRI

All patients were studied with a 1.5 T tomograph (Gyroscan NT Intera Release 12, Philips, Eindhoven, The Netherlands, maximum gradient strength 30 mT/m, peak slew rate 120mT/m/msec) using a four-channel receiver coil developed for upper abdomen examinations. Every patient was positioned in supine position with the arms extended over the head in order to reduce the artifacts. As recommended, we checked the accuracy of our scanner with an MR-DWI phantom study [27]. The standard upper abdomen MR protocol is reported in table 1.

table 1

Sequence Details

Sequence	TR/TE flip angle (degrees)	No. of b Values	NSA	Matrix	FOV (mm, AP-RL)	Slice thickness (mm)/number	Bandwidth (Hz/pixel)	Sense	AT (s)
T1w in/out phase[a]	231–121/ 14.6–2.3/80	NA	1	256 × 165	300–420	5/24	470	1,5	18
T1w (THRIVE)[b]	3.8/1.5/80	NA	1	256 × 169	350–400	4/40	560	1,5	16
T2w single-shot[c]	810/80	NA	1	256 × 165	300–420	5/40	260	NA	120
Dwl SSH EPI[d]	1800/66 /90	16	2	128 × 65	300–420	9/12	1739	NA	253

NA not applicable; THRIVE volumetric interpolated breath-hold examination. AT acquisition time (seconds).
[a]Axial T1-weighted 2D gradient echo in/out phase breath-hold sequence.
[b]T1-weighted 3D-GRE with volumetric interpolated breath-hold examination fat sat THRIVE sequences were performed before and repeated three times at 35–70–180 seconds intervals after the dynamic bolus injection of gadolinium chelate and at 20 minutes during hepatobiliary phase.
[c]Axial and coronal T2-weighted half-Fourier single-shot turbo spin-echo free- breath, intersection slice gap = 10%.
[d]DWI free-breathing, EPI single-shot, multi-b: 0-750 s/mm^2 (with 15 steps of 50 s/mm^2), TR/TE = msec, EPI factor = 65, intersection gap = 1 mm, half scan factor 73%.

In the volunteers (groups A-D) the MRI was performed without CA and DW sequences set as follows:

axial D-weighted echo planar (EPI) spin echo; singleshot, breath-hold sequence; b value 0–300 s/mm2 and 0– 1000 s/mm2; TR/TE=1343/42 ms and 1867/67 ms for b value 0–300 s/mm2 and 0–1000 s/mm2, respectively; EPI factor=39; slice thickness/number=9 mm/12; intersection slice gap=1 mm; flip angle=90°; sense factor 2; FOV=300–420 mm; NSA=2; half scan factor 62%; bandwidth 1976–1493 Hz for b value 0–300 and 0–1000 s/mm2, respectively; RFOV 70%; phase scan percentage 73%; acquisition voxel (mm3) 3.32/4.55/9.00; reconstructed voxel (mm3) 1.33/1.33/9.00; acquisition matrix 128×64;

reconstruction matrix 320×220; acquisition time=17 and 22 s for b value 0–300 and 0–1000 s/mm2, respectively; fat suppression obtained by spectral presaturation inversion recovery. Considering the

already demonstrated liver isotropy [32], only one diffusion gradient direction was applied in every acquisition in order to reduce the minimum available TE and consequently the unwanted T2 weighting of the DW sequence. The orientation of the diffusion gradient is defined by the option "gradient overplus" (Philips Medical System) and the corresponding ADC maps were calculated (b=0–300 s/mm2, b=0–1000 s/mm2). Moreover, a smaller cohort of 16 subjects out of 40 were submitted to a supplemental FB, multi-b, DWI acquisitions (16 b value, range 0–750 s/mm2, with steps of 50 s/mm2, table 1).

After gadoxetic acid administration, the 3D sequence was repeated during hepatic artery phase with a delay determined by the Care Bolus technique (mean delay time, about 30 sec). The acquisition was repeated again at 75 seconds during portal vein phase, during the equilibrium phase at 180 seconds, and during the hepatobiliary phase at 5, 10, 15, and 20 minutes. The Care Bolus technique in the sagittal and parasagittal orientations was used to determine the exact time to begin the artery phase acquisition, considering one scan per second: TR/TE=3.5/1.1 msec, slice thickness = 60 mm, intersection gap = 20%, field of view (FOV) = 400 mm, effective matrix size =128x128, NSA=2. The region of interest (ROI) with appropriate size was located in the abdominal aorta at the level of the celiac trunk. The Care Bolus reached the ROI level after 20–25 seconds, on average; we began the THRIVE sequence acquisition by an automatic breath-hold (expiratory) recorded voice command (given 6 sec in advance to the start of the acquisition). In these patients, 25 mmol/kg body weight of gadoxetic acid (then 1 mL per 10 kg weight) was administered at 1 mL/sec intravenously, as recommended, with a mechanical power injector (Spectris Solaris, MedRad, Indianola, PA) through a 20G catheter inserted into an antecubital vein, followed by a 20-mL saline flush at the same injection rate. Patients were monitored for 2 hours after the examination to observe any adverse

effects.

Methods of sampling

The DW images were evaluated by two radiologists and a physicist in consensus and then re-evaluated by the study coordinator (with 4, 6, 4 and 14 years of experience in DWI, respectively).

The data (mean and SD) were collected in Regions Of Interest (ROIs) of about 1200 pixels manually drawn in the middle part of the right liver, excluding the focal liver lesions and taking care that the signal intensity coefficient of variation inside the ROI was less than 10% at every b value. In "CA group" patients, three averaged ROIs were drawn twice (before and after CA administration) [27].

In five patients with focal nodular hyperplasia (FNH) we performed the DWI measurements also on the focal lesion between the 15' and 20' when the lesion was slightly more enhanced than the surrounding parenchyma [33].

DWI parameters

DW images were processed using the two-compartments model of Intra Voxel Incoherent Motion [31], represented by the following equation

$$\frac{S_b}{S_0} = (1 - PF)\exp(-bD) + PF\exp(-bD^*) \qquad (1)$$

where S0 and Sb are respectively the signal without and with the application of the diffusion gradient, PF is the fraction of water diffusing and flowing in the random oriented capillary network, 1-PF the fraction of extravascular water, D the slow diffusion coefficient and D* the fast diffusion coefficient, that models the slow and the fast Intra Voxel Incoherent Motion, respectively.

To determine PF, D and D* data were not simultaneously fitted over equation (1), given the high dispersion and the limited sampling of DWI signals at low b value (b < 150 s/mm2) [34,35], but a two step fitting procedure was adopted, as described in other papers [27,36, 37].

PF and D were estimated from signal intensity data at high b-values (b ≥ 200 s/mm2, where pseudodiffusion contribution is negligible) by fitting the equation

$$\frac{S_b}{S_0} = (1 - PF)\exp(-bD). \qquad (2)$$

The estimated values of PF and D were then reported in equation (1) and all multi-b (whole b range: 0 - 750 s/mm2) data were subsequently processed to estimate D*.

Finally ADC was estimated fitting data to the following equation (whole b range: 0 - 750 s/mm2):

$$\frac{S_b}{S_0} = \exp(-b \cdot ADC)$$

(3)

This two-steps fitting procedure was performed using a semiautomatic home-made software that drives the nonlinear regression algorithms provided in Gnuplot (http://www.gnuplot.info/, 4.4.2 release).

Statistical analysis

For the "age patients" group (healthy volunteers) the ANOVA test was performed to find differences among ADC group means. The Pearson's correlation coefficient (r) was obtained to investigate the association between ADC (b values 300 and 1000 s/mm^2 for BH acquisitions and 50, 100, 150, 300 s/mm^2 for FB acquisitions), PF, D, D* and age. The variation across all ages of all these DWI parameters was assessed in a linear regression model. In case of absence of significant correlation between DWI parameters and age, the mean, the SD, and the 95% limits of agreement of all the parameters were calculated including all the subjects.

For the "CA group" , the data was analyzed "per group" and "per patient".

All the subjects were divided into four groups, according to the different time of the second DWI acquisition (5, 10, 15, 20 minutes after gadolinium injection).

Mean and SD were calculated in each group for every DWI related parameters (PF, D, D*, ADC).

All the data were tested for normality by the Shapiro-Wilk test. In case of normal distribution at Shapiro-Wilk test, the Dunnet test was applied to compare all the groups with pre-CA group. Significance threshold was set at p=0.05.

Without a significant differences among groups , all the values of PF, D, D* and ADC, obtained before and after gadoxetic acid injection, were averaged by including the whole group of patients and by separating cirrhotic and non cirrhotic patients.

2.6. Results

The accuracy of the scanner was good (the long-term reproducibility of the ADC was 1%).

Forty healthy adult volunteers were included in the "age group" (27 males, 13 females, age range 26-86 years, mean age 48 years). The patients were homogeneously divided into 4 groups (A, B, C, and D) as described in Materials and Methods.

Twenty-eight patients were enrolled in the "CA group" (four of them were excluded because of non-cooperative behavior leading to strong movement artifacts on DW images). The remaining 24 patients (14 males, mean age 62 years, age range 25–84 years) were divided into 4 groups of six each, as described in Materials and Methods. Out of 24 patients, 13 were cirrhotic and 11 non cirrhotic. In particular, in 13 cases CA was administered for suspicion of hepatocellular carcinoma in cirrhosis (confirmed HCC in five cases). The other 11 patients underwent the examination for characterization/follow-up of lesions with previous computed tomography and/or ultrasound and resulted in one hemangioma, five FNH(s), two metastasis(es), while three exams were negative for focal lesions.

ADC mean, SD, and 95% confidence interval for "age group", on BH with b value=0–300 and 0–1000 s/mm^2 DW images, were calculated and reported for each group (table 2).

table 2

ADC values by age group

Group	b = 300 s/mm^2			b = 1000 s/mm^2		
	Mean	SD	95% CI	Mean	SD	95% CI
A	2747	567	2419–3074	1650	192	1539–1761
B	2686	472	2291–3081	1483	99	1400–1565
C	2783	650	2195–3282	1555	184	1396–1714
D	2742	800	2211–3356	1558	222	1496–1620

Apparent Diffusion Coefficient (ADC) mean, standard deviation (SD), 95% confidence interval (CI) for each group both at b = 300 and 1000 s/mm^2 (data in 10^{-6} mm^2/s).

ANOVA showed no significant differences in the mean ADC of the different groups (p=n.s.). No significant correlation between the subject's age and ADC was established, considering either BH or FB acquisition data, obtained at all the b values (50, 100, 150, 300, 1000 s/mm^2). No significant correlation with age was observed for PF, D and D*

evaluation. Pearson's correlation coefficient for all the DWI parameters, with statistical significance and 95% confidence interval, were reported (table 3).

table 3

PF, D, $D*$ and ADCs of healthy subjects and correlation with age

	Method (subj. n)	Mean	S.D.	Mean 95% CI	r	P	r 95% CI
PF	FB (16)	28.57	7.40	14.07–43.07	0.30	.26	−0.23 to 0.69
D	FB (16)	1090	140	816–1364	−0.28	.30	−0.68 to 0.25
$D*$	FB (16)	26728	9151	8792–44664	−0.27	.32	−0.67 to 0.26
ADC^{50}	FB (16)	3825	454	2935–4715	0.16	.67	−0.52 to 0.71
ADC^{100}	FB (16)	3333	388	2573–4093	0.39	.27	−0.32 to 0.81
ADC^{150}	FB (16)	2966	379	2223–3709	0.36	.31	−0.35 to 0.81
ADC^{300}	FB (16)	2238	251	1746–2730	0.50	.16	−0.13 to 0.87
ADC^{300}	BH (40)	2742	609	1548–3936	0.05	.74	−0.26 to 0.36
ADC^{1000}	BH (40)	1558	192	1182–1934	−0.2	.22	−0.48 to 0.08

PF (%), diffusion coefficient (D, in 10^{-6} mm^2/s), pseudodiffusion coefficient ($D*$, in 10^{-6} mm^2/s), ADCs (ADC^x, in 10^{-6} mm^2/s, where x indicates the b value in s/mm^2), mean, S.D., 95% confidence interval (CI) of healthy subjects, with the corresponding Pearson correlation coefficient with age (r, with statistical significance, P and 95% CI), varying the acquisition method (FB=free-breath, BH=breath-hold) and the number of subjects.

Fig. 1 and 2 show the scatterplots with linear regression line, respectively, of BH-ADC values and PF, D, D* vs. age. Given the absence of significant correlation between all the DWI parameters and age, mean, SD and 95% confidence interval of each DWI parameter were calculated including all the subjects belonging to each cohort (table 3).

fig.1
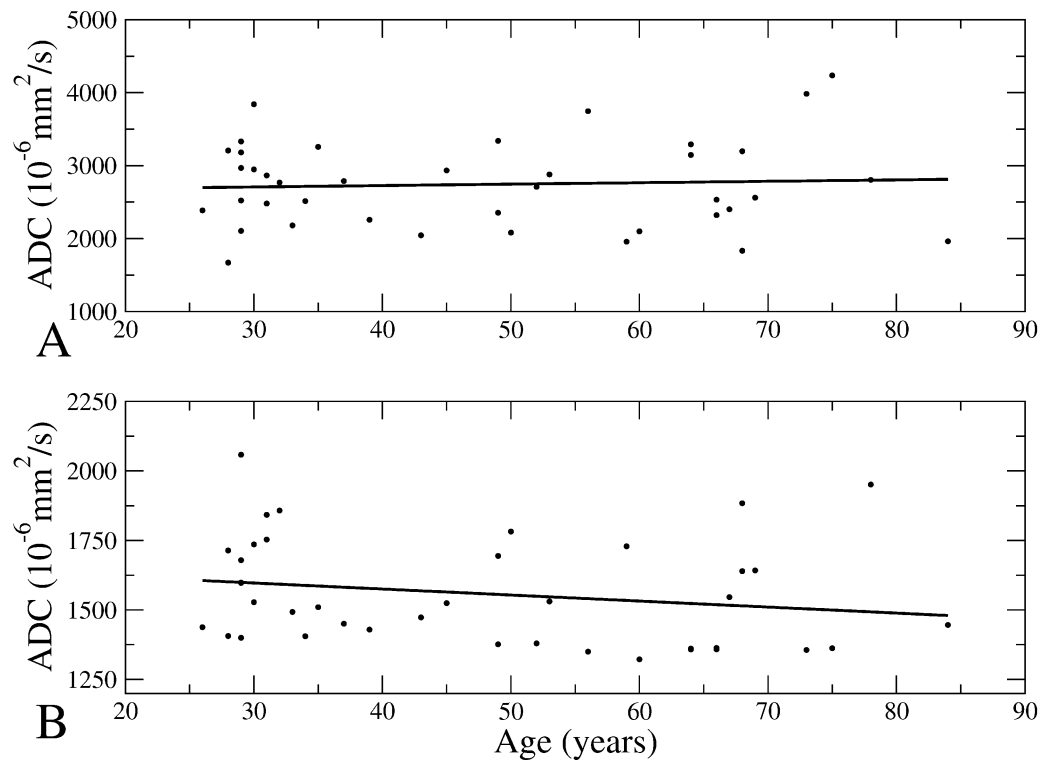
Breath-hold ADC vs. age with linear regression line. Data with b=300 (A; upper) and b=1000 s/mm2 (B; lower). The absence of a significant correlation between ADC and age, both in A and B, and the wide dispersion of data, more pronounced at b=300 s/mm2 (A), should be noted.

fig. 2
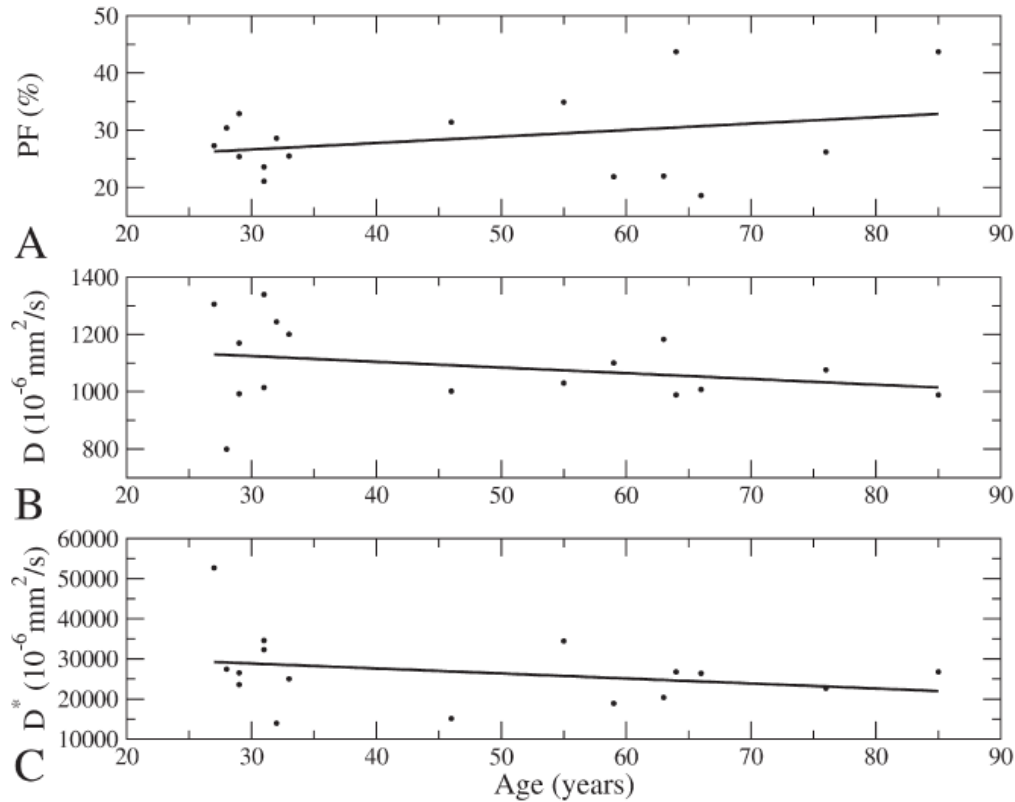
PF, D, D* vs. age with linear regression line. PF (A; upper), D (B; middle) and D* (C; lower) values. The absence of a significant correlation between PF,D, D* and age, both in A, B and C, should be noted.

Mean , SD of PF, D, D*, and fitted ADC of each group, belonging from the "CA group", are shown in table 4.
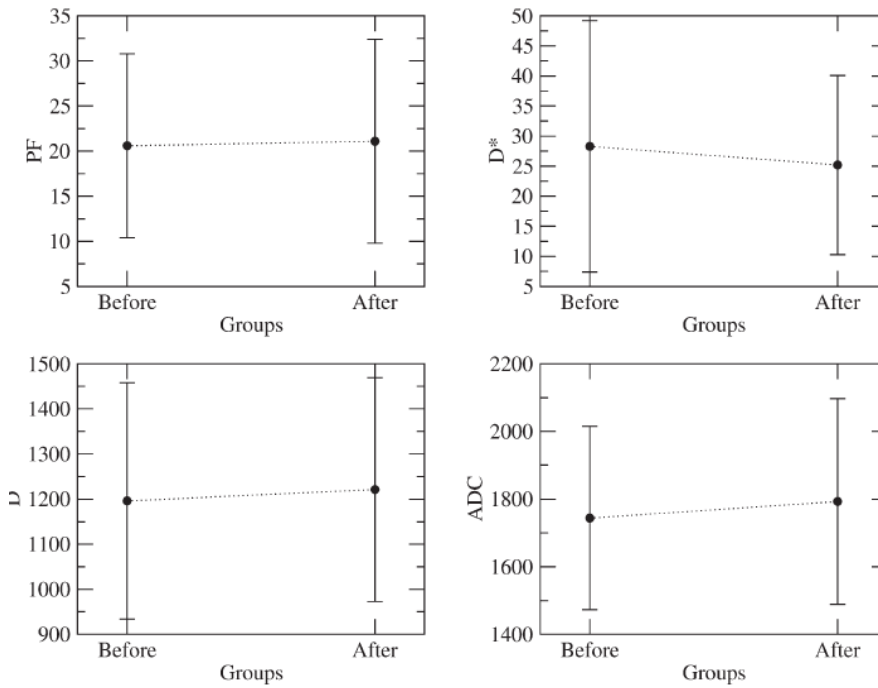
table 4

DWI Parameters in Each Group

	No MDC	5 min	10 min	15 min	20 min
PF	20.6±10.2	23.5±8.2	20.0±12.0	23.1±20.0	19.4±10.7
D	1196±262	1174±229	1312±306	1072±160	1248±190
D*	28.3±20.9	25.5±12.2	22.8±18.0	19.5±4.0	33.1±16.6
ADC	1744±271	1811±260	1840±244	1674±542	1786±236

Mean ± standard deviation (SD) of perfusion fraction (PF), diffusion coefficient (D, $\cdot 10^{-6}$ mm^2/s), pseudodiffusion coefficient (D*, $\cdot 10^{-3}$ mm^2/s) and apparent diffusion coefficient (ADC, $\cdot 10^{-6}$ mm^2/s) calculated in each group.

The Shapiro–Wilks test did not show any significant deviation from normality of each parameter distribution in each group, although with a low p value for D in the pre-CA and 10-minute groups (p= 0.09 and 0.12, respectively) and D* in the pre-CA group (p = 0.13). Dunnett's test did not show any significant difference of the averages of PF, D, D*, and ADC, comparing the pre-CA and the other post-CA groups (p> 0.30). The mean and SD of

PF, D, D*, and ADC calculated including data acquired before and after CA injection are reported (fig. 3).

fig. 3

Plot (mean±SD) of PF (percent), D ($\cdot$ 10^{-6} mm^2/s), D* ($\cdot 10^{-3}$ mm2/s), and ADC ($\cdot$ 10^{-6} mm^2/s) calculated using data acquired before and after the administration of contrast agent.

Data considering cirrhotic and non cirrhotic patients are reported (table 5): data pre- and post-CA administration are substantially similar, with a slight decrease in PF and ADC in cirrhotic group.

table 5

DWI Parameters in Patients With and Without Liver Cirrhosis

	Liver cirrhosis 11 patients		No liver cirrhosis 13 patients	
	Before CA injection	After CA injection	Before CA injection	After CA injection
PF	19.2±10	18.0±10	23.8±9	25.6±12
D	1214±289	1241±233	1155±190	1180±270
D*	31.8±21.4	31.3±29.2	28.0±18.6	29.6±21.7
ADC	1718±282	1706±262	1853±254	1910±305

Mean ± standard deviation (SD) of perfusion fraction (PF), diffusion coefficient (D,$\cdot$ 10^{-6} mm^2/s), pseudodiffusion coefficient (D*, $\cdot 10^{-3}$ mm2/s) and apparent diffusion coefficient (ADC,$\cdot$ 10^{-6} mm^2/s) calculated before and after CA administration in patients showing and not showing liver

cirrhosis, respectively. No significant differences were found among before and after CA administration values.

In the five patients with FNH(s), we observed that in the 20 minutes acquisition the focal lesion signal intensity (SI) in DWI was slightly higher with respect to the surrounding parenchyma. Thus, we performed an additional signal sampling for each patient, including in the ROI only the focal lesion. Afterwards PF, D, D*, and ADC were estimated considering the average signal of the FNH at every b value. The resulting maximum coefficient of variation, considering data acquired before and after CA injection, was =8% for PF, D, and ADC, while = 16% for D*.

2.7. Discussion

The DWI is certainly an interesting topic for its possible applications. In liver imaging many efforts have been made and are ongoing to establish a correlation between ADC measurements and liver changes. We firstly have investigated the correlation between age and ADC values of the liver without finding out any significant correlation, either at low-medium b values (FB acquisitions: 50–100–150–300 s/mm^2) or medium-high b values (BH acquisitions: 300–1000 s/mm^2).

It is well known that there is about 40% reduction in blood flow and a similar or slightly less reduction in liver mass during aging [38–41].

With a relevant reduction in liver blood flow, one would presume that there would be a decrease in ADC values with age, at least at lower b values. In our series, the width and asymmetry of ADC histograms (fig. 4) show that the ADC values are affected by a perfusion phenomenon, and that its spread is probably due to different components of flow and to a large variability in PFs.

fig. 4

A   B
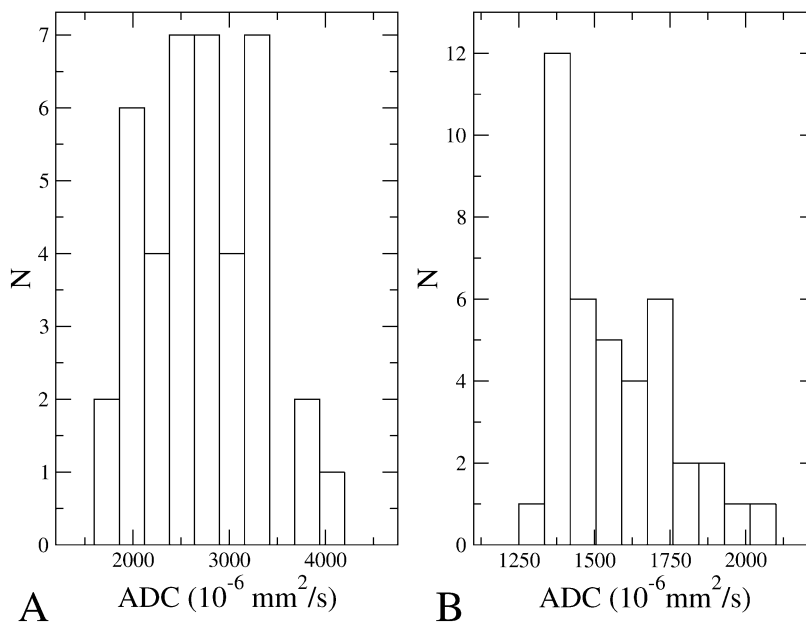
Histogram of breath-hold ADC values.
Data at b = 300 (bin size = 260 x 10^{-6} mm^2/s) (A-left) and b = 1000 s/mm^2 (bin size = 85 x 10^{-6} mm^2/s) (B-right). The higher ADC mean value at b=300 s/mm^2 (A) compared to b=1000 s/mm^2 (B) and the more symmetric shape of ADC distribution in (A) vs. (B) (skewness = 0.48 and 0.79, respectively) should be noted.

This probably also reflects the observed change in skewness between b=300 and b=1000 s/mm^2 ADC distributions and the symmetry of the D values distribution (0.48, 0.79 and 0.06, respectively). In fact, at high b values, the diffusion component is predominant in ADC measurements and the residual effect of perfusion probably contributes to the asymmetric right tail of the ADC histograms: the absence of asymmetry in the D values distribution support this hypothesis. This ADC stability during different ages offers the possibility to use, in the future, non-age-matched groups in studies on liver ADC. Furthermore, the documented wide range of liver parenchyma ADC values (at b=1000 s/mm^2) among healthy subjects, from around 1300 to 2000×10−6 mm^2/s (fig. 1), suggests that it is improbable that this technique provides a valid mean value as a reference for all or at least most of the subjects. We can argue that quantitative DWI seems more useful in following a single subject's disease over time and is therefore more appropriate for longitudinal rather than cross-sectional studies. In fact, recent literature reports have shown that ADC is not satisfactory for distinguishing different solid focal liver lesions [42,43] or grading fibrosis [13–14,44]. On the contrary, results of the studies devoted to the evaluation and follow-up of the response of metastatic liver tumors to chemotherapy are hopeful [45,46].

To better investigate possible age-related quantitative DWI variations, we examined also PF, D and D* in a smaller cohort of 16 volunteers (four for each age group), using a multi-b sequence with many D weightings, which allows an highly accurate representation of DWI signal decay. Interestingly, we did not find any significant correlation also with these non-b-linked parameters and age.

In a second group of patients we studied the effect of the CA on DWI-related parameters values (PF, D, D*, ADC) in patients undergoing abdominal contrast MRI to study the liver. In our series the parameters showed no significant differences before and after gadoxetic acidadministration at any time. Previous interesting articles demonstrated that there is no significant difference before and after administration of gadopentetate dimeglumine (Multihance) in the signal and contrast-to-noise ratio (CNR) of focal liver lesions and hepatic parenchyma [47-49]. Chiu et al. [47] found that gadoxetic acid administration does not compromise CNR and ADC of focal hepatic lesions, while Choi et al. [48] have shown that DWI after gadoxetic acid administration can be used as a substitute for unenhanced DWI without compromising the CNR and ADC of focal hepatic lesions. Kinner et al. [49] did not observe a significant difference regarding DWI in patients with cirrhosis before and

after CA injection. Previous studies suggest that it is possible to perform DWI studies after liver-specific CA administration without compromising the signal and CNR, and ADC values of the most frequent focal liver lesions. However, these studies were performed with 3T tomography, which is not used for liver/abdominal daily routine. Although, until now, DWI related parameters have not been explored. Therefore, in our study, we evaluated whether, the values of liver parenchyma DW-related parameters may change because of the use of gadoxetic acid, regardless of the patient or the disease studied. PF, D, D*, and fitted ADC, are less dependent on the choice of the acquisition b-values. The physiological interpretation proposed, for the first time, by Le Bihan et al. [4,5] is that D represents the slow diffusion coefficient, which describes thermal diffusion of water molecules (slow motion), while PF is the fraction of water molecules flowing inside the capillary network. Both can be estimated using a series of DW images with b >150–200 s/mm2 (in our series until 750 with steps of 50). In their model, Le Bihan et al., suggested, the coefficient D*, as an indicator of the influence of non diffusional intravoxel incoherent motion on the MR-DWI signal. The coefficient D* is related to the random flow within capillary network (fast motion), and depends on very low b-values (under 150) [5]. It should be underlined that D, PF, and D* are not automatically calculated as ADC. (maps obtained by commercial MR software using signal ratio from only two images, one with and one without D weighting). Differently, DWI parameters, are calculated by fitting the equations described by Le Bihan et al. The need for a more complex model, than the monoexponential ADC one, arose from the observation that, in a homogeneous phantom, a monoexponential signal decay was expected and registered, while it was not true on DW signals acquired in the liver parenchyma, where a biexponential signal behavior was observed [4]. In our study, PF, D, D*, and fitted ADC are parameters not directly depending on the D-weighting of the sequence (ie, on the b-value), increasing, as a consequence, the range of applicability of the results. While the aforesaid article [48] focused on focal liver lesions, we focused on the hepatic parenchyma. DWI changes related to other factors than the disease, such as age or the administration of CA [47].

As known, the liver SI increases after gadoxetic acid administration until the 30° minute; after that, SI slowly decreases [10,50,51]. This rise in SI and then in intracellular concentration might have caused some modifications in the DWI related parameters. Thus, we decided to measure their values at various time intervals (every 5 minutes). Our results show that it is possible to acquire quantitative DWI at every time after CA administration without affecting quantitative estimations. Since already studied by others [18,29], we did

not investigate the values in all the different focal liver lesions. It should to be taken into consideration that the structure with the maximum concentration of gadoxetic acid after dynamic scans is the liver parenchyma, with rare exceptions such as FNHs and well-differentiated HCCs in which biliary pole failures are present. For this reason we repeated the measures in a small pool of FNHs that demonstrated a SI higher than that measured in the surrounding parenchyma. Again, we found only small differences in PF, D, D*, and ADC calculated before and after CA administration. Moreover, the comparison between the PF, D, D*, and ADC values calculated on data acquired before and after CA administration was repeated, by dividing the patients into those with and without liver cirrhosis. Also in this sub-group analysis, we found only small differences. It must be underlined that these differences did not change the diagnostic power of PF and ADC: in fact, both are lower in patients affected by liver cirrhosis regardless of CA administration, as reported in table 5 than patients without cirrhosis. In particular, the reduction in PF observed in patients with diffuse liver disease could be explained with the reduction in capillary network observed in cirrhotic liver. It is also noteworthy that CA administration did not determine a bias in all the explored parameters, as shown by the recorded values (fig. 3). Finally, the SD of these parameters did not change after CA injection confirming the evidence that Gd-EOB-DTPA does not have a significant effect on DWI measurements.

In our opinion, the results of the present study, mainly the unchanged values of ADC before and after CA administration, are somewhat expected. In fact, the total amount of administered gadoxetic acid is very low (25 mmol/kg body weight) and its maximum blood concentration, measured immediately after bolus injection, is 0.2 mmol Gd/L. This very limited amount (a concentration 3 orders of magnitude lower with respect to water molecules flowing in the blood network) likely cannot alter the microscopic behavior of the water molecules, by means of its steric constraint. Moreover, it is known that all the Gd-chelates do not work as a linker but as a coordinator of the water molecules. This means that the water molecules are near, surrounding the Gd-chelate, tumbling around it, nevertheless remaining free and able to diffuse as happens in the absence of CA [50,51].

Our studies have some limitations that should be remarked. Firstly, the number of patients included in the study is limited. Secondly, in our scanner, echo-navigator technique is not available, and then we obtained multi-b sequence in FB modality, that is clearly less reproducible than that acquired with navigator. This is why slice locations of paired DW

acquisitions may not have been perfectly matched due to patient movement and breathing [52].

In conclusion, our studies indicate that there are no significant variations in liver DWI quantitative parameters (ADC, PF, D, and D*) depending on the age in healthy liver parenchyma or after gadoxetic acid administration.

3. References

1. Chung WS, Park MS, Shin SJ et al. Response Evaluation in Patients With Colorectal Liver Metastases: RECIST Version 1.1 Versus Modified CT Criteria. AJR 2012;199:809-815

2. Wang J, Wu N, Cham MD et al. Tumor response in patients with advanced non-small cell lung cancer: perfusion CT evaluation of chemotherapy and radiation therapy. AJR 2009; 193:1090–1096

3. Axel L. Cerebral blood flow determination by rapid-sequence computed tomography: theoretical analysis. Radiology 1980;137:679-686

4. Le Bihan D, Breton E, Lallemand D et al. MR imaging of intravoxel incoherent motions: application to diffusion and perfusion in neurologic disorders. Radiology 1986;161:401-407

5. Le Bihan D, Breton E, Lallemand D et al. Separation of diffusion and perfusion in intravoxel incoherent motion MR imaging. Radiology 1988;168:497-505

6. Pandharipande PV, Krinsky GA, Rusinek H, Lee VS. Perfusion imaging of the liver: current challenges and future goals. Radiology 2005;234:661-673

7. Bonekamp S, Corona-Villalobos CP, Kamel IR. Oncologic applications of diffusion-weighted MRI in the body. J Magn Reson Imaging. 2012;35:257-279

8. Kambadakone AR, Sahani DV.Body perfusion CT: technique, clinical applications, and advances. Radiol Clin North Am. 2009;47:161-178

9. Dawson P. Functional imaging in CT.Eur J Radiol. 2006;60:331-340

10. Qayyum A. Diffusion-weighted imaging in the abdomen and pelvis: concepts and applications. Radiographics 2009;29:1797–1810

11. Türkbey B, Aras Ö, Karabulut N, et al. Diffusion-weighted MRI for detecting and monitoring cancer: a review of current applications in body imaging. Diagn Interv Radiol 2012;18:46–59

12. Colagrande S, Pallotta S, Vanzulli A, Napolitano M, Villari N. The diffusion parameter in magnetic resonance: physics, techniques and semeiotics. Radiol Med 2005;109:1–16

13. Naganawa S, Kawai H, Fukatsu H, Sakurai Y, Aoki I, Mimiura S, et al. Diffusion-weighted imaging of the liver: technical challenges and prospects for the future. Magn Reson Med Sci 2005;4:175–186

14. Taouli B, Tolia AJ, Losada M et al. Diffusion-weighted MRI for quantification of liver fibrosis:preliminary experience. Am J Roentgenol 2007;189:799–806

15. Taouli B. Diffusion-weighted MR imaging for liver lesion characterization:a critical look. Radiology 2012;262:378–380

16. Taouli B, Sandberg A, Stemmer A et al. Diffusion-weighted imaging of the liver: comparison of navigator triggered and BH acquisitions. J Magn Reson Imaging 2009;30:561–568

17. Kwee TC, Takahara T, Koh DM, Nievelstein RA, Luijten PR. Comparison and reproducibility of ADC measurements in breath-hold, respiratory triggered, and free-breathing diffusion-weighted MR imaging of the liver. J Magn Reson Imaging 2008;28:1141–1148

18. Kandpal H, Sharma R, Madhusudhan KS, Kapoor KS. Respiratory triggered versus breath-hold diffusion-weighted MRI of the liver lesions: comparison of image quality and apparent diffusion coefficient values. AJR Am J Roentgenol 2009;192:915–922

19. Schraml C, Nina FS, Clasen S. Navigator respiratory-triggered diffusion-weighted imaging in the follow-up after hepatic radiofrequency ablation-initial results. J Magn Reson Imaging 2009;29:1308–1316

20. Braithwaite AC, Dale BM, Boll DT, Merkle EM. Short- and mid-term reproducibility of apparent diffusion coefficient measurements at 3.0-T diffusion-weighted imaging of the abdomen. Radiology 2009;250:459–465

21. Conturo TE, McKinstry RC, Aronovitz JA, Neil JJ. Diffusion MRI: precision, accuracy and flow effects. NMR Biomed 1995;8:307–332

22. Colagrande S, Belli G, Politi LS, Mannelli L, Pasquinelli F, Villari N. The influence of diffusion and relaxation-related factors on signal intensity: an introductive guide to magnetic resonance diffusionweighted imaging studies. J Comput Assist Tomogr 2008;32:463–474

23. Kwee TC, Takahara T, Niwa T, et al. Influence of cardiac motion on diffusionweighted magnetic resonance imaging of the liver. Magn Reson Mater Phys 2009;22:319–325

24. Le Bihan D. Intavoxel incoherent motion perfusion MR imaging: a wake up call. Radiology 2008;249:748–752

25. Murtz P, Flacke S, Traber F, van den Brink JS, Gieseke J, Schild HH. Abdomen: diffusion-weighted MR imaging with pulse-triggered single-shot sequences. Radiology 2002;224:258–264

26. Padhani AR, Liu G, Mu-Koh D, et al. Diffusion-weighted magnetic resonance imaging as a cancer biomarker: consensus and recommendations. Neoplasia 2009;11:102–125

27. Colagrande S, Pasquinelli F, Mazzoni LN, Belli G, Virgili G. MR diffusion weighted imaging of healthy liver parenchyma: repeatability and reproducibility of apparent diffusion coefficient measurement. J Magn Reson Imaging 2010;31:912–920

28. Karabulut N, Elmas N. Contrast agents used in MR imaging of the liver. Diagn Interv Radiol 2006;12:22–30

29. Saito K, Araki Y, Park J, et al. Effect of Gd-EOB-DTPA on T2-weighted and diffusion-weighted images for the diagnosis of hepatocellular carcinoma. J Magn Reson Imaging 2010;32:229–234

30. Ahn SJ, Kim MJ, Hong HS, et al. Distinguishing hemangiomas from malignant solid hepatic lesions: a comparison of heavily T2-weighted images obtained before and after administration of gadoxetic acid. J Magn Reson Imaging 2011;34:310–317

31. Tamada T, Ito K, Yoshida K, et al. T2-weighted magnetic resonance imaging of the liver: evaluation of the effect in signal intensity after Gd-EOB-DTPA enhancement. J Comput Assist Tomogr 2010;34:182–186

32. Taouli B, Vilgrain VR, Dumont E, Daire JL, Fan B, Menu Y. Evaluation of liver diffusion isotropy and characterization of focal hepatic lesions with two single-shot echo-planar MR imaging sequences: prospective study in 66 patients. Radiology 2003;226:71–78

33. Grazioli L, Bondioni MP, Haradome H, et al. Hepatocellular adenoma and focal nodular hyperplasia: value of gadoxetic acidenhanced MR imaging in differential diagnosis. Radiology 2012; 262:520–529

34. Patel J, Sigmund EE, Rusinek H, Oei M, Babb JS, Taouli B. Diagnosis of cirrhosis with intravoxel incoherent motion diffusion MRI and dynamic contrast-enhanced MRI alone and in combination: preliminary experience. J Magn Reson Imaging 2010;31:589–600

35. Istratov AA, Vyvenko OF. Exponential analysis in physical phenomena. Rev Sci Instrum 1999;70:1233–1257

36. Callot V, Bennett E, Decking UK, Balaban RS, Wen H. In vivo study of microcirculation in canine myocardium using the IVIM method. Magn Reson Med 2003;50:531–540

37. Wirestam R, Borg M, Brockstedt S, Lindgren A, Holtas S, Stahlberg F. Perfusion-related parameters in intravoxel incoherent motion MR imaging compared with CBV and CBF measured by dynamic susceptibility-contrast MR technique. Acta Radiol 2001;42:123–128

38. Schmucker DL. Age-related changes in liver structure and function: implications for disease? Exp Gerontol 2005;40:650–659

39. Le Couteur DG, McLean AJ. The aging liver: drug clearance and an oxygen diffusion barrier hypothesis. Clin Pharmacokinetics 1998;34:359–373

40. Zeek J, Paltt D. Age related changes in the liver. Consequences for drug therapy. Fortschr Med 1990;30:651–653

41. Ito Y, Sørensen KK, Bethea NW, et al. Age-related changes in the hepatic microcirculation in mice. Exp Gerontol 2007;42:789–797

42. Sandrasegaran K, Akisik FM, Lin C, Tahir B, Rajan J, Aisen AM. The value of diffusion-weighted imaging in characterizing focal liver masses. Acad Radiol 2009;16:1208–1214

43. Parikh T, Drew SJ, Lee VS, Wong S, Hecht EM, babb JS, Taouli B. Focal liver lesion detection and characterization with diffusionweighted MR imaging: comparison with standard breath-hold T2-weighted imaging. Radiology 2008;246:812–822

44. Talwalkar JA, Yin M, Fidler JL, Sanderson SO, Kamath PS, Ehman RL. Magnetic resonance imaging of hepatic fibrosis: emerging clinical applications. Hepatology 2008;47:332–342

45. Cui Y, Zhang XP, Sun YS, Tang L, Shen L. Apparent diffusion coefficient: potential imaging biomarker for prediction and early detection of response to chemotherapy in hepaticmetastases. Radiology 2008; 248:894–900

46. Marugami N, Tanaka T, Kitano S, et al. Early detection of therapeutic response to hepatic arterial infusion chemotherapy of liver metastases from colorectal cancer using diffusion-weighted MR imaging. Cardiovasc Intervent Radiol 2009;32:638–646

47. Holzapfel K, Bruegel M, Eiber M, et al. Characterization of small (b≤10 mm) focal liver lesions: value of respiratory-triggered echoplanar diffusion-weighted MR imaging. Eur J Radiol 2010;76:89–95